Geophysical Research Letters

Supporting information for

Incision of submarine channels over pockmark trains in the South China Sea

Kaiqi Yu[1, 2, 3], Elda Miramontes[4, 5], Tiago M. Alves[6], Wei Li[1, 2, 3 *], Linlin Liang[3, 7], Shuang Li[1, 2, 3], Wenhuan Zhan[1, 2, 3], and Shiguo Wu[3, 8]

[1]Key Laboratory of Ocean and Marginal Sea Geology, South China Sea Institute of Oceanology, Innovation Academy of South China Sea Ecology and Environmental Engineering, Chinese Academy of Sciences, Guangzhou 510301, China.

[2]Southern Marine Science and Engineering Guangdong Laboratory (Guangzhou), Guangzhou 511458, China.

[3]University of Chinese Academy of Sciences, Beijing 100049, China.

[4]Faculty of Geosciences, University of Bremen, Bremen 28359, Germany.

[5]MARUM-Center for Marine Environmental Sciences, University of Bremen, Bremen, 28359, Germany.

[6]3D Seismic Laboratory, School of Earth and Ocean Environmental Sciences, Cardiff University, Main Building, Park Place, Cardiff, CF10 3AT, United Kingdom.

[7]State Key Laboratory of Tropical Oceanography, South China Sea Institute of Oceanology, Chinese Academy of Sciences, Guangzhou, China.

[8]Institute of Deep-sea Science and Engineering, Chinese Academy of Sciences, Sanya, 572000, China.

*Corresponding authors: Dr. Wei Li (wli@scsio.ac.cn)

Contents

Introduction

The uninterpreted seismic profiles (Figures S1 and S2) shown in Figures 1c and 3 are provided as supporting information to this study. They show details of the seismic architecture of investigated channels. We also show a map with the location of all available seismic data interpreted in this study (Figure S3). Eight supplementary seismic profiles are provided for a more comprehensive analysis of pockmarks, alongslope and across-slope channels (Figures S4-S6). These seismic profiles highlight morphological differences among alongslope and across-slope channels. Diagrams explaining how channels and pockmarks were measured are provided in Figures S7 and S8. The speed profiles of ocean currents in western South China Sea are provided in Figure S9. Finally, Table S1 provides morphological details of the alongslope and across-slope channels highlighted in Figure 2.

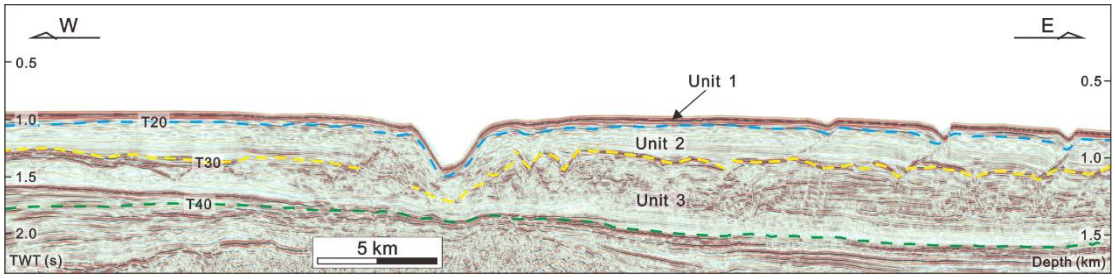

Figure S1. Interpretation of the seismic profile shown in Figure 1c. This study focuses on shallow strata in the western South China Sea, which are subdivided into three units: Unit 1 (Quaternary); Unit 2 (Pliocene) and Unit 3 (Late Miocene). The bases of these seismic-stratigraphic units correlate with seismic horizons T20, T30 and T40, respectively. The amplitude and continuity of seismic reflections show significant differences when comparing near-seafloor strata to the deeper units imaged in seismic data.

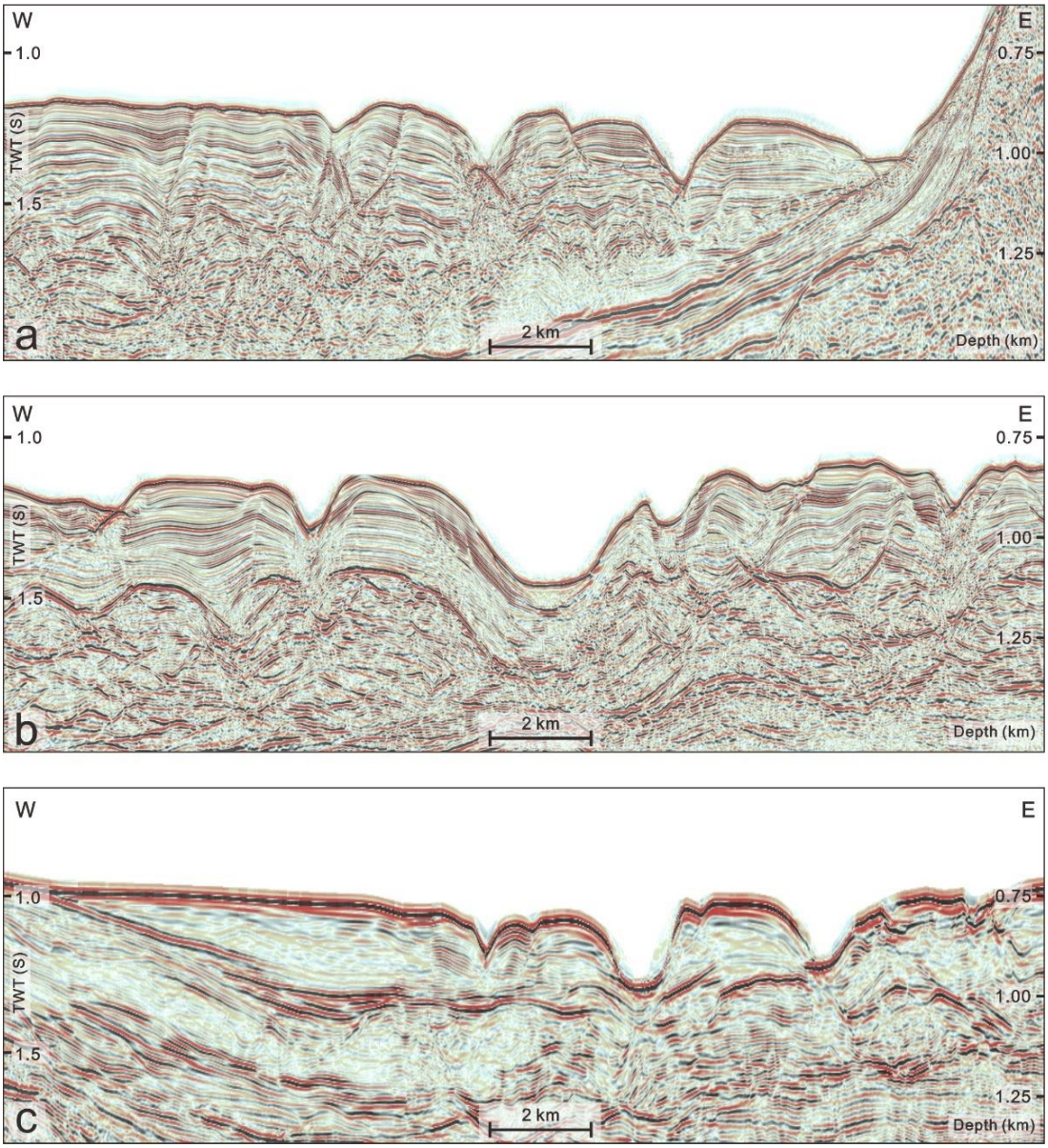

Figure S2. Uninterpreted versions of the seismic profiles shown in Figure 3. Seismic facies in the figure are markedly variable at depth. The seismic reflections close to the seafloor are parallel and continuous, but chaotic when moving deeper into the imaged succession.

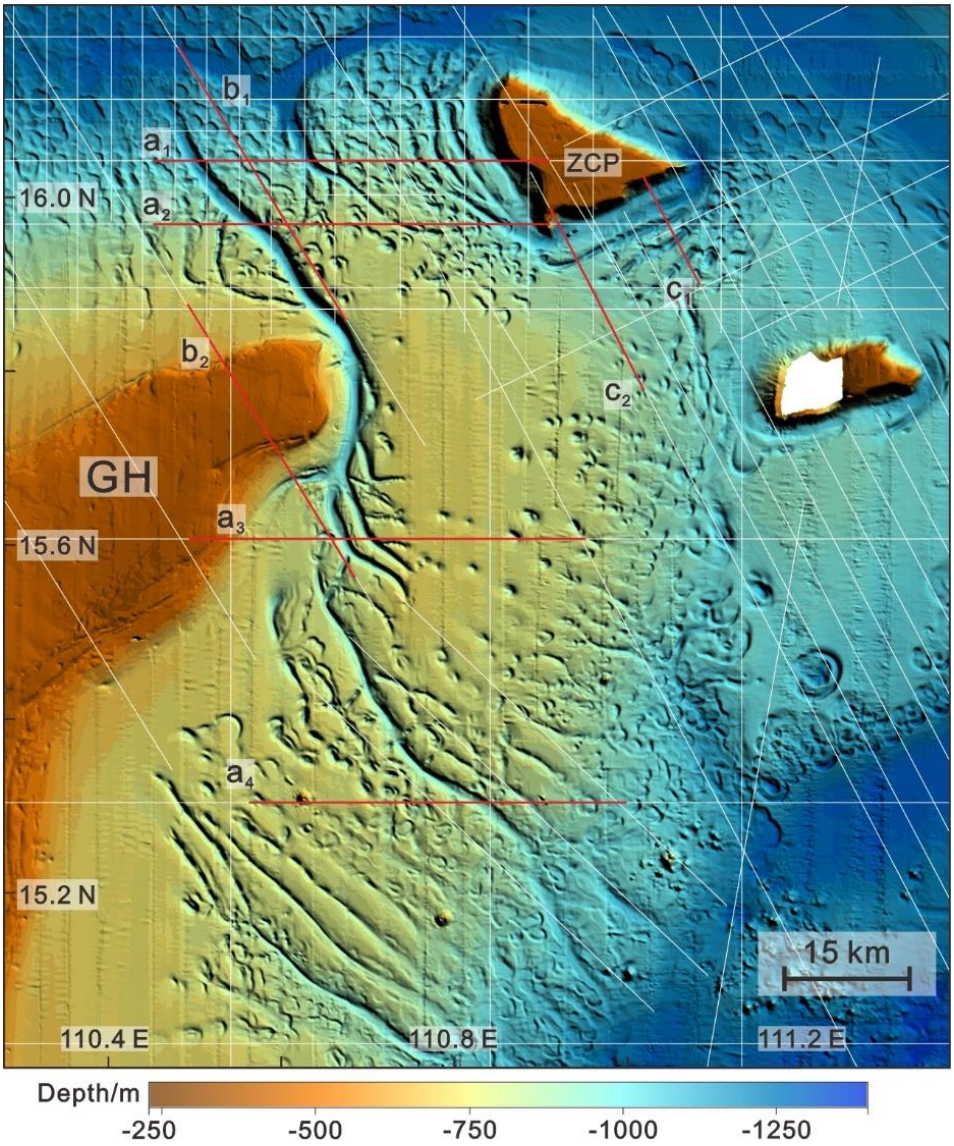

Figure S3. Bathymetric map of the study area highlighting the locations of the seismic profiles interpreted in this study (see white solid lines). The supplementary seismic profiles provided are labelled and shown by the red solid lines.

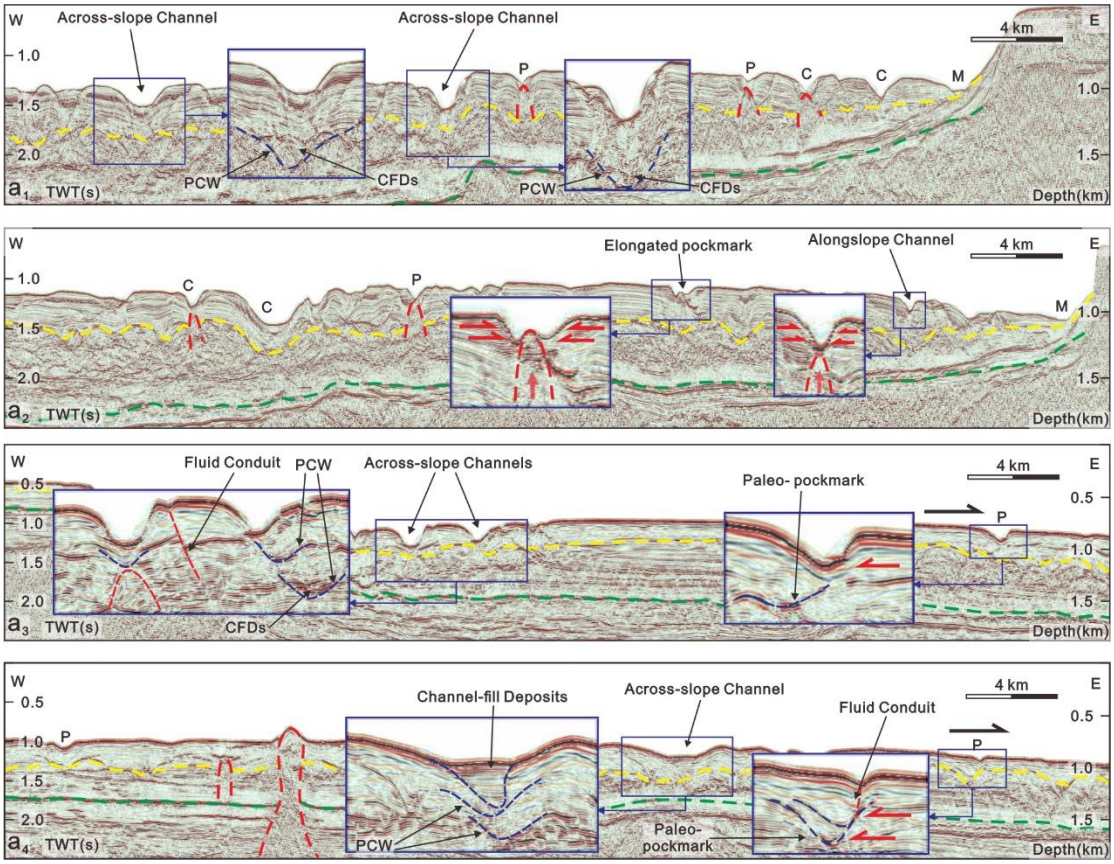

Figure S4. W-E seismic profiles (a_1, a_2, a_3 and a_4) highlighting the main morphological differences among across-slope and alongslope channels. The location of the four seismic profiles is shown in Figure S3. Yellow and green dashed lines indicate the bases of Pliocene (T30) and Late Miocene (T40) strata. The red dashed lines highlighting the presence of fluid escape features in the study area. Black horizontal arrows point out to the downslope direction. P: Pockmark; C: Channel; M: Moat; PCW: Paleo-channel wall; CFDs: Channel-fill Deposits; Zoomed-in insets show details of channels and pockmarks.

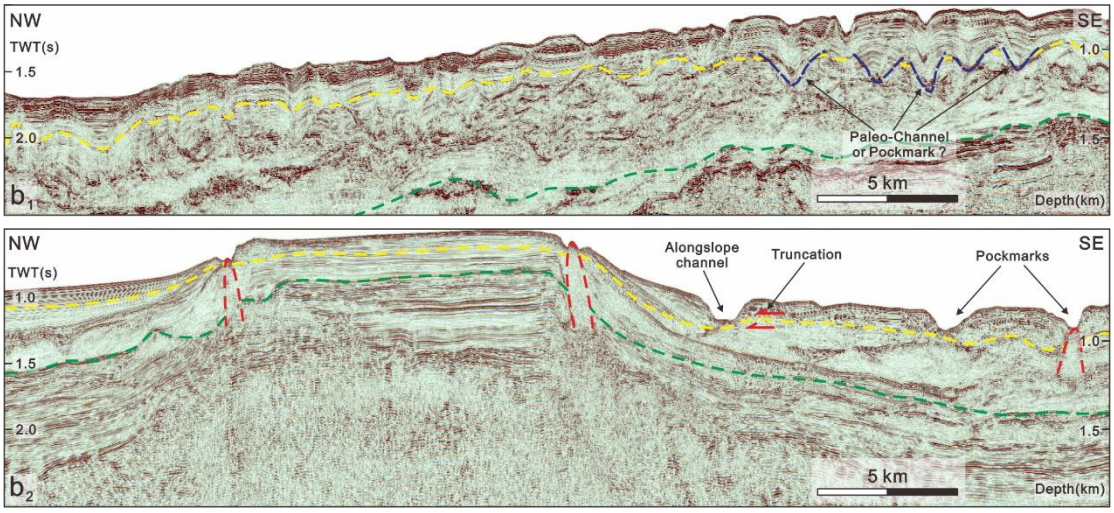

Figure S5. NW-SE seismic profiles revealing the seismic stratigraphy across the Guangle High (GH) and along the channel D-D' (shown in Figure 2c). The yellow and green dashed lines indicate the bases of Pliocene (T30) and Late Miocene (T40) strata. The red dashed lines highlight the presence of fluid escape features. Many paleo-channels (or paleo-pockmarks) are identified in the upper reaches of channel D-D', and truncate horizon T30 (Pliocene). The flanks of the GH are eroded by alongslope channels, as indicated by the erosional truncations shown in the seismic profile. See Figure S3 for the location of the two seismic profiles.

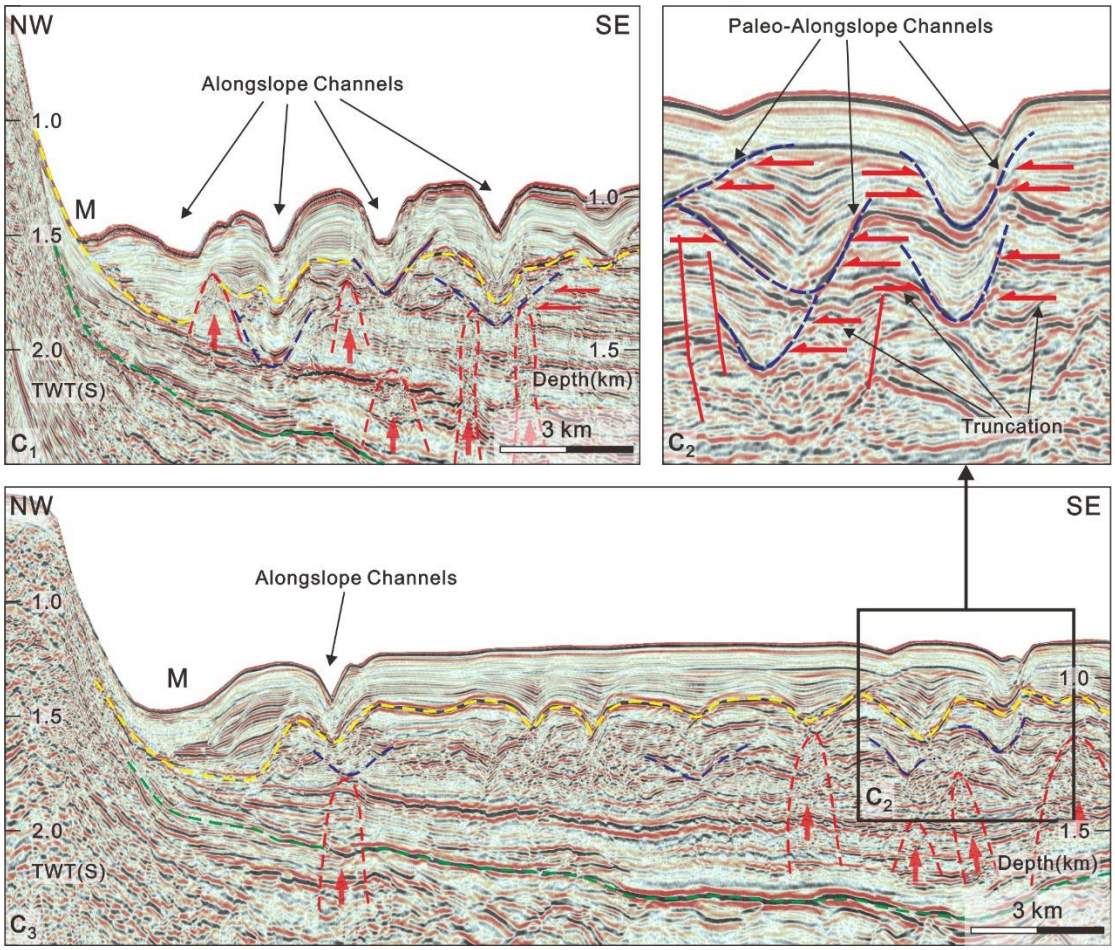

Figure S6. Seismic profiles oriented perpendicularly to the southeastern slope of the Zhongjianbei Carbonate Platform (ZCP). They highlight the cross-section morphology of the alongslope channels that are parallel to the slopes flanking the ZCP. The zoomed-in inset highlights the morphology of older alongslope channels. The bases of Pliocene (T30) and Late Miocene (T40) strata are indicated by the yellow and green dashed lines. Many paleo-channels and paleo-pockmarks (highlighted by the dark blue dashed lines) are identified below the modern channels, modern pockmarks and the seafloor. Older alongslope channels show erosional truncation on their flanks as indicated by the horizontal red arrows. Fluid escape features (shown as red dashed lines) originate from strata under horizon T30 or T40, revealing a close relationship with the channels and pockmarks above. M-moat. The location of the seismic profiles is shown in Figure S3.

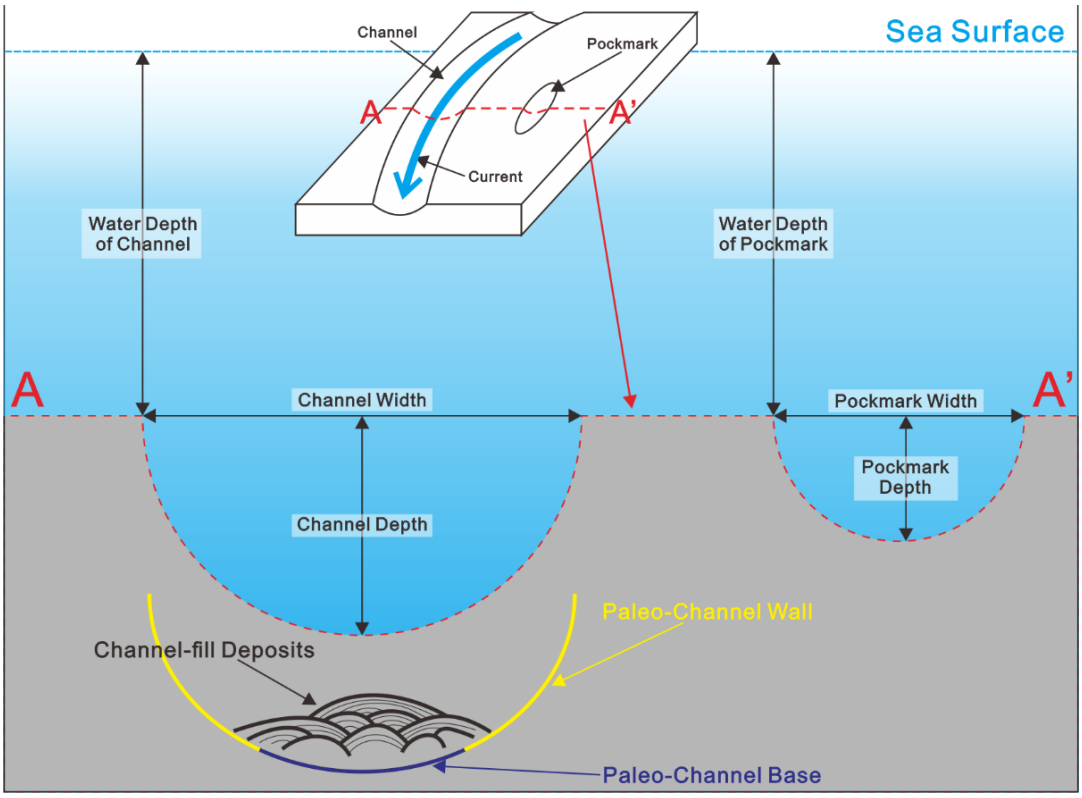

Figure S7. Diagram summarizing the definitions of water depth of channel and pockmark, depth and width of channel and pockmark, paleo-channel wall and base, channel-fill deposits used in this study.

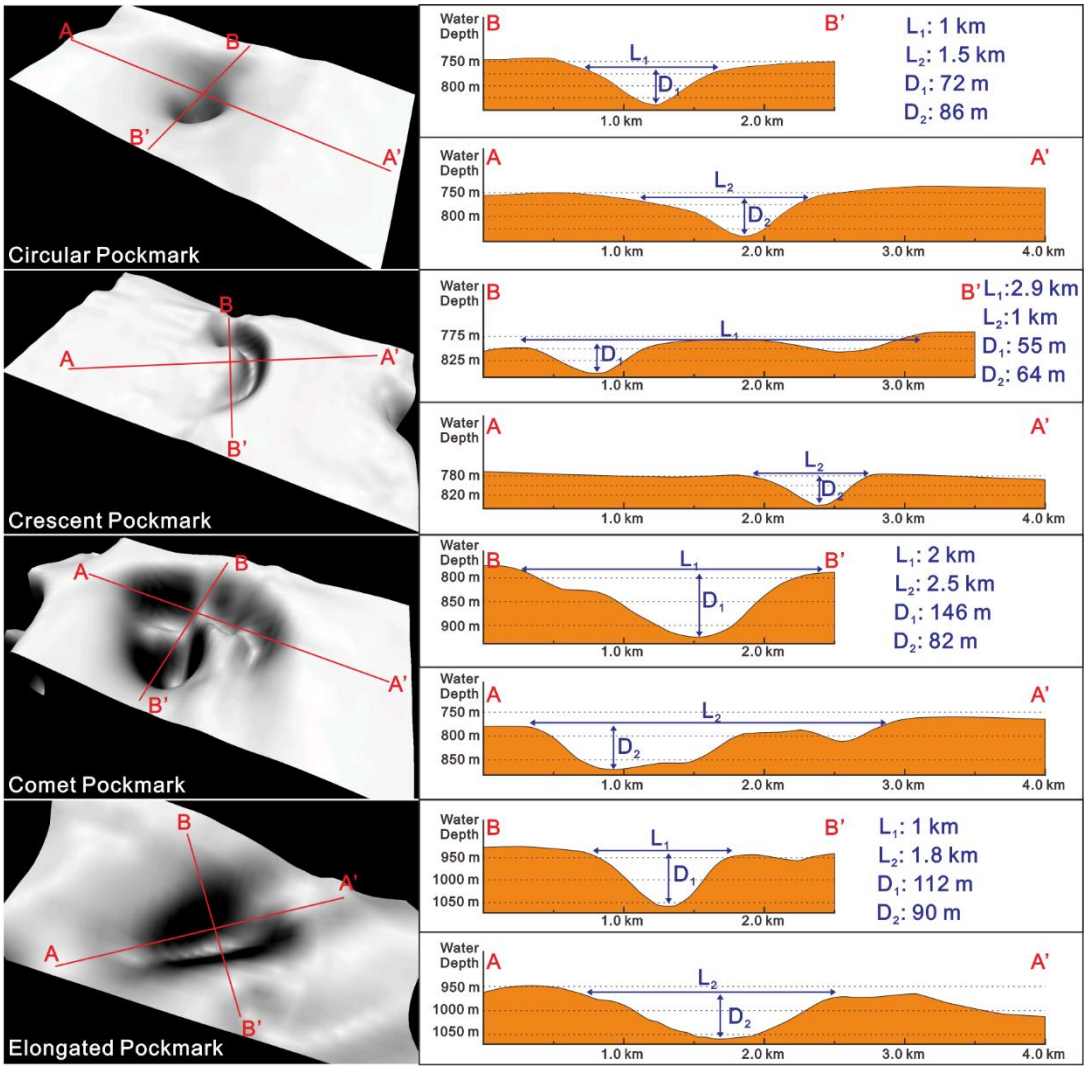

Figure S8. Morphological data for circular, crescent, comet and elongated pockmarks in the study area.

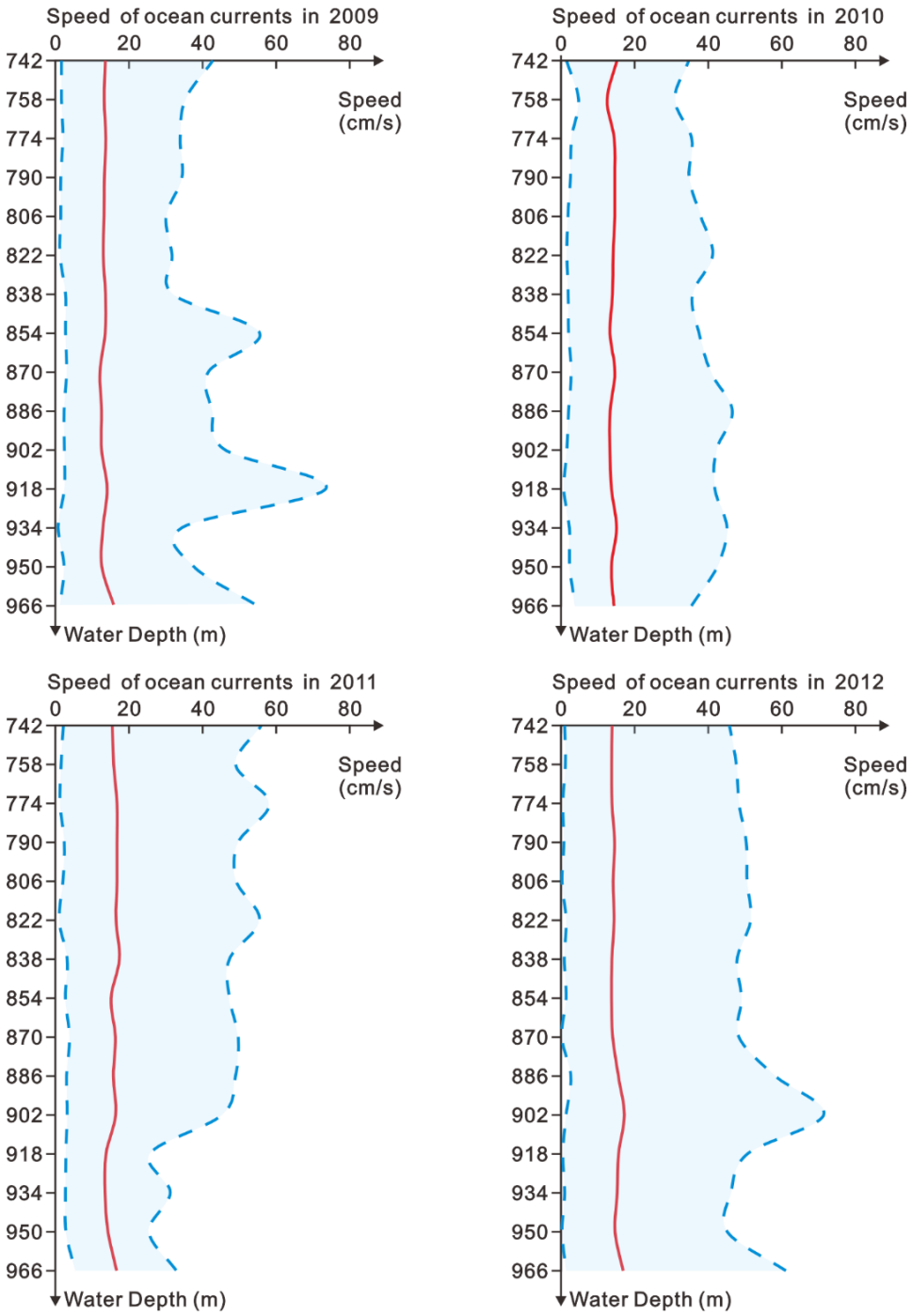

Figure S9. Profiles show the speed of ocean currents between the water depth of 742 and 966 m, acquired with a vessel-mounted ADCP Ocean Surveyor 38 kHz in the western South China Sea (2009-2012) obtained from Yang et al. (2019). The red lines indicate the average value of the in-situ measured current speed at different water depths, with the locations shown in Figure 1a. The blue dashed lines in the left and right reveal the minimum and maximum value of current speed at these locations, respectively. The speed profiles reveal a complex water circulation, with average speeds ranging between 10 to 20 cm/s and maximum speeds reaching 80 cm/s, at water depths typical of the study area.

Table S1. Detailed morphological information for the alongslope and across-slope channels imaged in Figure 2d.

Channel	A-A'	B-B'	C-C'	D-D'	E-E'	F-F'	G-G'
Classification	Along-slope channel	Along-slope channel	Along-slope channel	Across-slope channel	Across-slope channel	Along-slope channel	Across-slope channel
Maturity	Mature stage	Immature stage	Intermediate stage	Mature stage	Immature stage	Mature stage	Intermediate stage
Channel depth (average)	73 m	80 m	94 m	240 m	92 m	171 m	129 m
Channel width (average)	1.7 km	1.2 km	1.3 km	2.6 km	1.1 km	2.6 km	1.9 km
Water depth (average)	950 m	917 m	980 m	798 m	770 m	745 m	802 m
Gradient of channel thalweg	0.51°	0.19°	0.40°	0.12°	0.85°	0.15°	0.17°
Roughness of thalweg (R_z*)	15 m	43 m	32 m	9 m	40 m	15 m	37 m

***Ps.** *the calculation of Roughness of thalweg (Rz) is based on the methodology of Sancaktar and Gomatam (2001):*

$$R_z = \frac{Z_1 + Z_2 + \cdots + Z_{n-1} + Z_n}{n}$$

References

Sancaktar, E., & Gomatam, R. (2001). A study on the effects of surface roughness on the strength of single lap joints. Journal of Adhesion Science and Technology, 15(1), 97–117. https://doi.org/10.1163/156856101743346

Yang, Y., Xu, C., Li, S. & He, Y. (2019). Ship-mounted ADCP dataset of scientific investigation over the South China Sea (2009 – 2012). (V1). 2019-03-08. https://doi.org/10.11922/csdata.2019.0006.zh